IOP Conf. Series: Journal of Physics: Conf. Series **879** (2017) 012024 doi:10.1088/1742-6596/879/1/012024

Thermodynamics of ultra-sonic cavitation bubbles in flotation ore processes.

Royer[1] J J, Monnin[1] N, Pailot-Bonnetat[1] N, Filippov[1,2] L O, Filippova[1,2] I V, Lyubimova[2] T

[1]Université de Lorraine, GeoRessources, ENSG, 2 rue Doyen Marcel Roubault, BP10162, F-54505, Vandœuvre-lès-Nancy, France.
[2]National University of Science and technology "MISIS", 117049 Moscou, Russia
[3]Perm State University, Perm, Russia.

Email: jean.jacques.royer@gmail.com

Abstract. Ultra-sonic enhanced flotation ore process is a more efficient technique for ore recovery than classical flotation method. A classical simplified analytical Navier-Stokes model is used to predict the effect of the ultrasonic waves on the cavitations bubble behaviour. Then, a thermodynamics approach estimates the temperature and pressure inside a bubble, and investigates the energy exchanges between flotation liquid and gas bubbles. Several gas models (including ideal gas, Soave-Redlich-Kwong, and Peng-Robinson) assuming polytropic transformations (from isothermal to adiabatic) are used to predict the evolution of the internal pressure and temperature inside the bubble during the ultrasonic treatment, together with the energy and heat exchanges between the gas and the surrounding fluid. Numerical simulation illustrates the suggest theory. If the theory is verified experimentally, it predicts an increase of the temperature and pressure inside the bubbles. Preliminary ultrasonic flotation results performed on a potash ore seem to confirm the theory.

1. Introduction

Froth flotation is a widely commonly used effective process in mineral processing ([1], [2], [3]), wastewater cleaning [4], coal industry [5], and hydrocarbon pollution remediation [1]. The ability of air bubbles to selectively adhere to specific mineral surfaces and separating hydrophobic from hydrophilic materials ([1], [6]) makes froth flotation an effective technique widely used in the industry. Recent works have investigated froth flotation enhanced by ultrasonic stimulation ([3], [7]). In the previous paper [8], we have investigated the ultra sonic stimulation on flotation both at micro and macro scales showing that the overall flotation recovery increases due to an increase in bubble ability for capturing particles, especially because of higher particle-bubble collision and particle-bubble attachment probabilities.

In this work, we focused on the thermo-dynamical aspects induced by ultra-sonic treatment at the bubble scale assuming the same model for ultra sonic wave as in [8] i.e. the theoretical oscillating bubble radius time dependent curves is modeled by a trigonometric polynomial previously ([9], [10]). A thermodynamics approach is suggested to model the energy exchanges between the liquid and the gas bubble submitted to an ultrasonic treatment; the temperature and pressure behavior of a bubble is then calculated together with the internal energy, total work, and heat exchange assuming various gas models (including polytropic process, Soave-Redlich-Kwong, Peng-Robinson, and ideal gas). It is shown that the application of ultrasonic external fields increases the temperature and pressure of the gas trapped in bubbles.

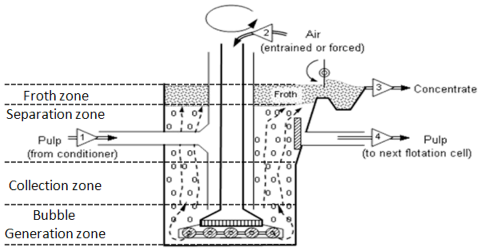

Figure 1. (a) Schematic cross-section with the different zones: 1 - the pulp enters the cell from a conditioner, and flows to the bottom of the cell; 2 - small air bubbles are passed down as a vertical impeller; 3 - collection of the mineral concentrate froth from the top of the cell; 4 - pulp flows to another cell. (Modified after http://www.wikiwand.com/en/Froth_flotation).

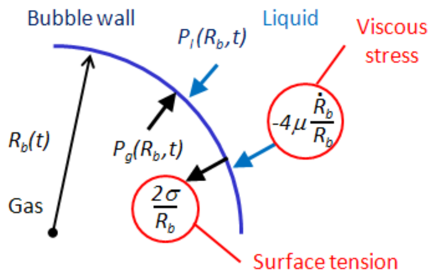

Figure 2. Schematic view of bubble-particle interaction and forces acting on the bubble surface including the gas surface tension, the liquid viscous stress, the liquid pressure P_l, the gas pressure P_g, t is time, R_b the bubble radius, $\dot{\boldsymbol{R}}_{\boldsymbol{b}}$ its derivate against time, μ the cinematic liquid viscosity, and σ surface tension (after [11])

2. Governing equations for bubble evolution under ultrasonic waves

Hydrodynamics of single bubble immersed in a liquid subjected to ultrasonic waves can be described by the Navier-Stokes equations applied to the gas inside the bubble, initially at rest, and to the incompressible liquid adjacent to the bubble wall. The Navier-Stokes equations can be solved analytically in spherical coordinates [9] or numerically using a radial formulation [10].

2.1. *Solving Navier-Stokes equations*

A bubble at rest with mean initial radius R_0, at pressure P_0, and temperature T_0, is immersed in an unbounded incompressible liquid submitted to an external time-dependent pressure at its boundary $P_\infty(t)=P_0+P(t)$, where t the time, and $P(t)$ the time-dependent pressure time (including negative and positive fluctuations). Far from the bubble the temperature of the liquid is assumed to be constant at T_∞. It is also assumed that the pressure and the temperature inside the bubble are always uniform, and therefore is time-dependant. The viscous Newtonian fluid is assumed incompressible with constant density ρ. The bubble has a spherical shape preserved during all the process, with radius $R(t)$ oscillating through time under ultrasound. Neglecting gravitational forces, the Navier-Stokes equations (or mass and momentum conservation equations) describe the flow field surrounding the bubble [10]. The first one is the continuity of the liquid:

$$\left(\frac{\partial \rho}{\partial t}\right) + \boldsymbol{\nabla}.\left(\rho\,\mathbf{u}(r,t)\right) = 0 \tag{1}$$

with $\boldsymbol{u}$ the liquid velocity, r the radial distance to the bubble center, and t the time. As the bubble is assumed to be spherical, Eq.(1) can be simplified into $\partial\,(r^2\,u(r,t)) = 0$ using spherical coordinates, with solution for the radial velocity:

$$u(r,t) = \frac{1}{r^2}F(t) \tag{2}$$

where $F(t)$ is a function of time determined by the boundary conditions. Assuming no mass transfer across the bubble boundary, the wall velocity in a local coordinate system attached to the bubble is equal to the change rate of its radius $u(R_b,t) = \dot{R}_b$ (where $\dot{R}_b$ is the derivation of R_b against time t), thus $F(t) = R_b^2(t)\dot{R}_b$, and consequently Eq.(2) becomes:

$$u(r,t) = \left(\frac{R_b(t)}{r}\right)^2 \dot{R}_b \tag{3}$$

Neglecting the dynamic viscosity of the liquid, and substituting the radial component of the velocity, the radial component of the Navier-Stokes equation applicable to the liquid can be written as:

$$\frac{1}{\rho}\frac{\partial P_l}{\partial r} + \frac{\partial u}{\partial t} + u(r,t)\frac{\partial u}{\partial r} = 0 \qquad -\frac{1}{\rho}\frac{\partial P_l}{\partial r} = \frac{R_b^2\,\ddot{R}_b + 2\,R_b\,\dot{R}_b^2}{r^2} - \frac{2\,R_b^4\,\dot{R}_b^2}{r^5}$$

$$\Rightarrow -\frac{1}{\rho}\int_{P_l(R_b,t)}^{P_\infty(t)} dP = \int_{R_b}^{\infty}\left(\frac{R_b^2\,\ddot{R}_b + 2\,R_b\,\dot{R}_b^2}{r^2} - \frac{2\,R_b^4\,\dot{R}_b^2}{r^5}\right)dr \Rightarrow \frac{P_l(R_b,t)-P_\infty}{\rho} = R_b\ddot{R}_b + \frac{3}{2}\,\dot{R}_b^2 \tag{4}$$

where $P_l(R_b, t)$ is the liquid pressure on the bubble wall which is equal to the sum of all forces acting on the wall bubble (Figure 2): (i) the *gas pressure* in the bubble P_g, (ii) the *viscous stress* σ_{rr} of the liquid; and (iii) the *superficial tension* τ. It comes $P_l = \sigma_{rr} + \tau + P_g$. The radial component of the *viscous stress* σ_{rr} acting on the bubble wall depends on the liquid cinematic viscosity μ [12]:

$$\sigma_{rr}(r,t) = 2\mu\,\frac{\partial u}{\partial \mathrm{r}} = -\,4\mu\,\frac{\dot{R}_b}{R_b(\mathrm{t})} \qquad (5)$$

The *surface tension* τ acting in the bubble is given by the Laplace's formula $\tau(t) = -\frac{2\sigma}{R_b(t)}$ where σ is the surface tension. A process for an ideal gas is *polytropic* and obeys the relation $PV^m = B$ if the ratio of energy transfers as heat δQ to energy transfer as work δW remains constant ($\delta Q/\delta W = cst = K$) at each infinitesimal step, m is the *polytropic coefficient* which depends on the nature of the process (and of the gas). For ideal gas, specific values of m vary between *isothermal* ($m = 1$) to *isentropic* (adiabatic or reversible) ($m = \gamma = 1.4$ for air), γ being the *adiabatic coefficient*. Assuming an ideal gas polytropic transformation for the gas trapped in the bubble, the gas pressure is equal to:

$$P_g(\mathrm{t}) = P_{g_0}\left(\frac{R_{b_0}}{R_b(\mathrm{t})}\right)^{3\mathrm{m}} \qquad (6)$$

with P_{g_0} the initial gas pressure in the bubble at rest. Assuming that at $t = 0$, $P_l(R_b,0) = P_0$ and $\dot{R}_b = 0$, the initial pressure in the bubble becomes $P_{g_0} = \frac{2\sigma}{R_{b_0}} + P_0$. Then, from Eqs. (5), and (6), the total pressure at the bubble boundary P_l can be written as:

$$P_l(R_b, \mathrm{t}) = \left(\frac{2\sigma}{R_{b_0}} + P_0\right)\left(\frac{R_{b_0}}{R_b(\mathrm{t})}\right)^{3\mathrm{m}} - 4\mu\,\frac{\dot{R}_b}{R_b(\mathrm{t})} - \frac{2\sigma}{R_b(t)} \qquad (7)$$

Other gas models (including ideal gas, Soave-Redlich-Kwong, and Peng-Robinson) can be used to predict the evolution of the internal bubble pressure (see §2.3.).

2.2. *Effect of ultra sound on the bubble pressure boundary*

From $P_\infty(t) = P_0 + P(t)$, and equating Eqs.(4) and (6), the time-dependent pressure term $P(t)$ is equal to:

$$P(t) = \left(\frac{2\sigma}{R_{b_0}} + P_0\right)\left(\frac{R_{b_0}}{R_b(\mathrm{t})}\right)^{3\mathrm{m}} - \frac{2\sigma}{R_b(t)} - \rho\left[R_b\ddot{R}_b + \frac{4\mu}{\rho}\frac{\dot{R}_b}{R_b} + \frac{3}{2}\,\dot{R}_b^2\right] - P_0 \qquad (8)$$

The general model can be used to describe the time evolution of the bubble radius $R_b(t)$ given by $R_b(t) = R_{b_0}f(t)$ with $f(\omega t) = 1 + \varrho\cos(\omega(t+\tau_0) + \upsilon\pi/2)\,\{1 - \mu'\,[1 - \exp\{\sin(\omega(t+\tau_0))\}]\}$ with $\varrho < 1$, where the coefficients (R/R_0, ϱ, $\omega\tau_0$, $\nu = \mu' = 1$) are constant or function of the Deborah number D_e ($R/R_0(D_e)$, $\varrho(D_e)$, $\omega\tau_0(D_e)$, $\nu = \mu' = 0$) [7], where $D_e = \lambda\omega$ (with λ the polymer relaxation time) [10]. Thus, Eq.(8) can be rewritten as:

$$P(t) = \left(\frac{2\sigma f^{-1}}{R_{b_0}} + P_0\right)[\mathrm{f}^{-3\mathrm{m}+1} - 1] + P_0 f^{-3m}[1 - f] - \rho R_{b_0}^2\left[f\,\ddot{f} + \frac{4\mu}{\rho R_{b_0}^2}\dot{f}f^{-1} + \frac{3}{2}\dot{f}^2\right] \qquad (9)$$

Eq.(9) gives explicitly the time-dependent pressure term $P(t)$ as a function of the ultra sonic wave function f.

2.3. *Pressure inside the bubble*

Eq.(9) gives the pressure of the liquid at the bubble boundary assuming a polytropic process for the ideal gas trapped in the bubble. Several other gas models (including Soave-Redlich-Kwong, and Peng-Robinson) can be used to predict the evolution of the internal bubble pressure.

Polytropic ideal gas process: (P): $P_g(t)\ V_b(t)^m = P_{g0}\ V_{b0}{}^m = B$ where B is a constant, as $V_b(t) = 4/3\pi R^3{}_b(t)$, reporting all constant terms in B', it comes: $P_g(t)\ R_b(t)^{3m} = P_{g0}\ R_{b0}{}^{3m} = B'$ (with $B' = 3B/4\pi$), then using the general model for describing the time-dependent bubble radius submitted to ultrasound, the gas pressure inside the bubble is given by: $P_g(t) = \left(\frac{2\sigma}{R_{b_0}} + P_0\right)\mathrm{f}^{-3\mathrm{m}}$.

Soave-Redlich-Kwong gas model (SRK): $P_g(t) = \frac{\mathcal{R}\mathrm{T_b(t)}}{\mathrm{V_m - b}} - \frac{\mathrm{a}\alpha}{\mathrm{V_m(V_m + b)}}$ with $a = \frac{0.427\mathcal{R}^2\mathrm{T_c^2}}{\mathrm{P_c}}$; $\mathrm{b} = \frac{0.08664\mathcal{R}\mathrm{T_c}}{\mathrm{P_c}}$ where T_c and P_c are the critical temperature and pressure for the gas, respectively (for air $V_m = 22.4$l.mol^{-1}), and $\mathfrak{R} = 8.314$ J.(K·mol)$^{-1} \approx 2$ cal.(K·mol)$^{-1}$ is the ideal gas constant.

Normally, $\alpha = (1 + (0.48508 + 1.55171\omega - 0.15613\omega^2)(1 - T_r^{0.5}))^2$ with ω the *acentric factor*, and T_r the dimensionless temperature T_r (t) = $T_b(t)/T_c$. Assuming no change of state in the bubble, the acentric factor can be neglected, so a simplified expression for $\alpha = (1 + 0.48508(1 - T_r^{0.5}))^2$ can be used.

Peng-Robinson gas model (PR) is similar to the SRK model $P_g(t) = \frac{\mathcal{R}T_b(t)}{V_m - b} - \frac{a'\alpha}{V_m(V_m + 2b') - b'^2}$ with $a' = \frac{0.457235\mathcal{R}^2 T_c^2}{P_c}$; $b' = \frac{0.077796\mathcal{R}T_c}{P_c}$; $\alpha = (1 + \kappa(1 - T_r^{0.5}))^2$ with $\kappa = 0.37464 + 1.54226\omega - 0.26992\omega^2$, but neglecting the acentric factor gives: $\alpha = (1 + 0.37464(1 - T_r^{0.5}))^2$. The temperature $T_b(t)$ can be calculated using the polytropic model.

Generalized SRK-PR model: The SRK and PR model can be rewritten in a single equation: $P_g(t) = \frac{\mathcal{R}T_b(t)}{V_m - b} - K$ where $K = K_{SRK} = \frac{a\alpha}{V_m(V_m + b)}$, and $K = K_{PR} = \frac{a\prime\alpha}{V_m(V_m + 2b') - b'^2}$, for the SRK and PR models.

2.4. Temperature inside the bubble

A *polytropic* transformation for an *ideal* gas model is assumed for estimating the uniform temperature inside a homogeneous gas bubble.

Polytropic process: $T_b(t)\, V_b(t)^{m-1} = T_{b0}\, V_{b0}^{\ m-1} = C$ (from reporting the ideal gas equation $PV = n\Re T$ in the definition $PV^m = B$), where the constant $C = B/n\Re$; as for pressure, it comes: $T_b(t) = T_{b0} f^{3(1-m)}$.

Ideal gas model (I) : $P_g(t)\, V_b(t) = n\Re\, T_b(t)$ and $P_{g0}\, V_{b0} = n\Re\, T_{b0}$ where n is the amount of gas (in moles), $\Re$ = 8.314 J.(K·mol)$^{-1}$ being the ideal gas constant (equal to the product of the Boltzmann constant and the Avogadro constant). When ultra sounds are applied, it comes: $T_b(t) = T_{b_0} f^{3(1-m)} \left(\frac{2\sigma}{R_{b_0} P_0} + 1\right)$ with a pressure equal to $P_g(t) = P_{g_0} f^{-3m} \left(\frac{2\sigma}{R_{b_0} P_0} + 1\right)$.

2.5. Temperature in the liquid around the bubble

The fluid temperature T_l around the bubble is given by the heat equation in spherical coordinates:

$$\frac{\partial T_l}{\partial t} = \frac{\alpha_l}{r^2}\frac{\partial}{\partial r}\left(r^2 \frac{\partial T_l}{\partial r}\right) - u(r,t)\frac{\partial T_l}{\partial r} \tag{10}$$

where α_l is the liquid thermal diffusivity, u(r,t) the fluid radial velocity around the bubble, and T_l the liquid temperature. Due to the nonlinearities, this equation has no exact analytic solutions. However, a relevant approximation of the solution valid when the thickness of the thermal boundary layer surrounding the bubble is small compared to its radius is given by [13]:

$$T_\infty(t) - T_B(t) = \sqrt{\frac{\alpha_l}{\pi}} \int_0^t \frac{R_b^2(x)\left(\frac{\partial T}{\partial r}\right)_{r=R_b(x)}}{\sqrt{\int_x^t R_b(y)^4 dy}} dx \tag{11}$$

An approximation of the analytical solution can be found if the bubble surface is assumed to be maintained at constant temperature. Assuming that the spherical bubble with a constant average radius R_{b0} and a constant average temperature $\tilde{T}_B$ at the bubble surface, is placed at rest in a stagnant fluid at constant temperature $\tilde{T}_f$ (far away from the bubble), the average temperature $\tilde{T}(r)$ in the surrounding fluid is an inverse distance function of the distance r to the bubble center given by [14] $\frac{\tilde{T}(r) - \tilde{T}_f}{\tilde{T}_B - \tilde{T}_f} = \frac{R_{b_0}}{r}$. Notice that the temperature profile is not dependent on the fluid thermal conductivity. The decrease in temperature is very fast locally, for small bubbles (around *100μm*), at a distance $r = 10R$ (*1mm*), the liquid temperature increases only of about *3°C* for a temperature difference of $\Delta T = \tilde{T}_B - \tilde{T}_f \approx 30°C$.

3. Energy balance and thermodynamic considerations

The energy balance in a bubble evolving under an external field such as ultrasonic treatment can be now calculated assuming a polytropic transformation and considering different gas models (Ideal, SRK, and PR). The first law of thermodynamics gives the total variation of the internal energy ΔU_{tot} of a system as the sum of the total work W_{tot} and the total heat Q_{tot} supplied to or escaping from the system through its boundaries: $\Delta U_{tot} = W_{tot} + Q_{tot}$.

Table 1. Synthesis of theoretical formula and results from various numerical experiments

	State equations		
Parameters	Ideal gas	Soave-Redlich-Kwong	Peng-Robinson
$T_b(t)$	$T_b(t) = T_{b_0} \mathrm{f}^{3(1-\mathrm{m})}\left(\frac{2\sigma}{R_{b_0}P_0}+1\right)$	$T_b(t) = T_{b0} f^{3(1-m)}$	
$\tilde{T}_b(in °C)$	$88.02°C$	$61.62°C$	
$\tilde{T}_b(in\ \mathrm{K})$	$361.17K$	$334.77K$	
$P_g(t)$	$\mathrm{P_g(t)} = \frac{n\mathcal{R}\mathrm{T_b(t)}}{\mathrm{V_b(t)}}$	$\mathrm{P_g(t)} = \frac{\mathcal{R}\mathrm{T_b(t)}}{\mathrm{V_m - b}} - \frac{\mathrm{a\alpha}}{\mathrm{V_m(V_m+b)}}$	$\mathrm{P_g(t)} = \frac{\mathcal{R}\mathrm{T_b(t)}}{\mathrm{V_m - b}} - \frac{\mathrm{a'\alpha}}{\mathrm{V_m(V_m+2b') - b'^2}}$
$\tilde{P}_g(in\ MPa)$	0.158	0.124	
$W_{tot}(t)$	$W_{tot}(t) = W_0\left[f^{3(1-m)}-1\right]$	$W_{tot}(t) = W_0\left[f^{3(2-m)} - f_0^{3(2-m)}\right]$; $W_0 = \frac{(m-1)n\mathcal{R}\,T_{b_0}}{m\,(m-2)}$	
$\widetilde{W}_{tot}(in\ 10^{-8}\ \mathrm{J})$	0.087	62	
$Q_{tot}(t)$	$Q_{tot}(t) = Q_0\left[f^{3(1-m)}-1\right]$	$Q_{tot}(t) = 4\pi Q_0 t\, f\left(f^{3(1-m)}-1\right)$; $Q_0 = k\,R_{b_0}T_{b_0}$	
$\tilde{Q}_{tot}(in\ 10^{-8}\ \mathrm{J})$	0.13	14.2	
$\Delta U_{tot}\ (t)$	$\Delta U_{tot}(t) = (W_0+Q_0)\left[f^{3(1-m)}-1\right]$	$\Delta U_{tot}(t) = W_{tot}(t) + Q_{tot}(t)$	
$\Delta U_{tot}\ (in\ 10^{-8}\ \mathrm{J})$	0.217	76.2	

3.1. Polytropic models (P)

Internal energy of a bubble: for an ideal gas $dU = nc_V\, dT_g = \frac{n\mathcal{R}\,\mathrm{d}T_g}{\gamma-1} = \frac{n\mathcal{R}\,T_g}{\gamma-1}(1-m)\frac{dV_b}{V_b}$ where n is the number of moles of gas, c_V is the molar constant volume (c_P pressure) heat capacity of the gas, and $\gamma = c_P/c_V$ the heat capacity ratio (γ =5/3 = 1.67 for monatomic gas with three degree of freedom, and 7/5 = 1.4 for diatomic gas with five degree of freedom, γ = 1.4 for air). After some arithmetic, it comes: $\Delta U_{tot} = \frac{P_{g_2}V_2 - P_{g_1}V_1}{\gamma-1} = U_0\left[f^{3(1-m)}-1\right]$, with $U_0 = \frac{V_0P_0}{\gamma-1}\left(\frac{2\sigma}{R_{b_0}P_0}+1\right)$. If the transformation is isothermal ($m=1$), and the total internal energy variation is null ΔU =0 (adiabatic transformation).

Total work: Assuming a polytropic process so $P_g(t)\ V_b(t)^m = P_{g0}\ V_{b0}{}^m$, the total work done by the system when the volume bubble changes from V_1 to V_2, is given by: $W_{tot} = -B\int_1^2 P_g(t)dV = -B\int_1^2 \frac{dV}{V^m(t)}$. For integration, one must separate the *isothermal* ($m=1$) to the *non-isothermal* ($m\neq1$) cases; it gives after some arithmetic: $m = 1$, $W_{tot} = B\ln\left(\frac{V_1}{V_2}\right)$; $m\neq1$ $W_{tot} = \frac{P_{g_2}V_2 - P_{g_1}V_1}{m-1}$. The total work can be rewritten in terms of temperature as: $W_{tot} = \frac{n\,\mathcal{R}\,(T_2-T_1)}{m-1}$. Finally, reporting in the total work expression the bubble pressure $P_g(t)$ for an ideal gas polytropic process, and $V_b(t) = 4/3\pi R^3{}_b(t)$, it comes: $m\neq1$, $W_{tot} = W_0\left[f^{3(1-m)}-1\right]$ where $W_0 = \frac{V_0P_0}{m-1}\left(\frac{2\sigma}{R_{b_0}P_0}+1\right)$ with V_0, P_0, T_0 are the volume, pressure, and temperature of the bubble at rest; for the isothermal case ($m=1$), $W_{tot} = -\,W_0'\ln(f)$ with $W_0' = 3n\mathcal{R}\,T_0$.

Heat supplied by the liquid Q_{tot} can be evaluated applying the first law of thermodynamics, for $m\neq1$ $Q_{tot} = \Delta U_{tot} - W_{tot} = (U_0 - W_0)\left[f^{3(1-m)}-1\right] = Q_0\left[f^{3(1-m)}-1\right]$, with $Q_0 = V_0P_0\left(\frac{2\sigma}{R_{b_0}P_0}+1\right)\left(\frac{1}{\gamma-1}-\frac{1}{m-1}\right)$. For an isothermal transformation ($m=1$) $Q_{tot} = -\,W_{tot} = W_0'\ln(f)$; when $m = \gamma = 1.4$, the transformation is adiabatic as the total heat supplied to the system is null ($Q_{tot} = 0$), $\Delta U_{tot} = W_{tot}$.

3.2. Generalized SRK-PR models with m≠1 *(isothermal case excluded)*

Total work: assuming a polytropic transformation, the gas pressure P_g and the bubble volume V_b are related by $P_g(t)\ V_b(t)^m = P_{g0}\ V_{b0}{}^m = C$; reporting the pressure given by the generalized SRK-PR gas state equation, it comes: $\left(\frac{\mathcal{R}\mathrm{T_b(t)}}{\mathrm{V_m-b}} - K\right)V_b^m(t) = C$. By differentiation $dV_b = -\frac{\mathcal{R}V_b(t)dT_b}{m(\mathcal{R}T_b(t) - K(V_m-b))}$.

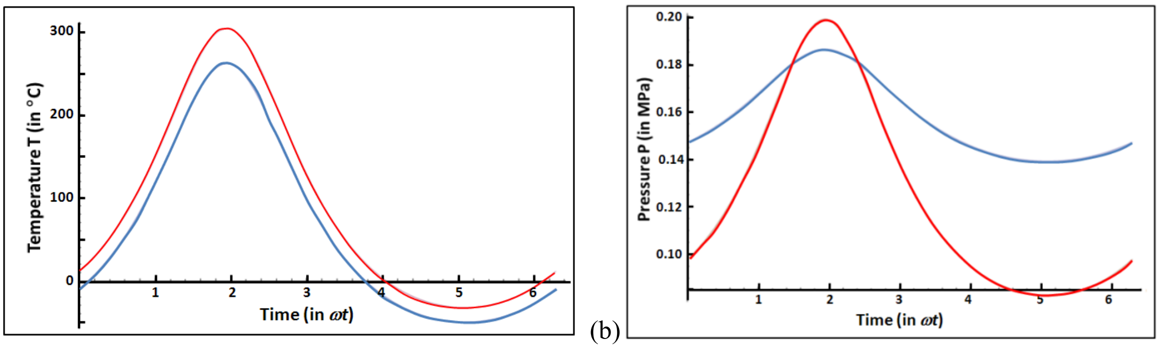

(a) (b)

Figure 3. (a) Calculated temperature inside a bubble for ideal (red), and polytropic (blue) gas model; (b) calculated pressure inside a bubble for ideal (blue), and SRK-PR (red) gas model. Average increase in temperature is about 43ºC, and pressure variation about 0.022 *MPa*.

So the total work is given by $W_{tot} = -\int_1^2 P_g(t)dV_b = \int_1^2 \left(\frac{\mathcal{R}V_b}{m(V_m-b)}\right)dT_b$, but as bubbles are spherical, $V_m - b \approx 4/3\pi R^3_{b0}$ so $\frac{V_b}{(V_m-b)} \approx \left(\frac{R_b(t)}{R_{b_0}}\right)^3 = f^3$; however, $dT_b = 3(1-m)T_{b_0}f^{2-3m}df$ so by integration, the total work is equal to: $W_{tot} = W_0\left[f^{3(2-m)} - f_0^{3(2-m)}\right]$ with $W_0 = \frac{(m-1)\mathcal{R}\,T_{b_0}}{m\,(m-2)}$ (valid for a molar volume, $n=1$), where f_0 is the f function at initial time $t=0$.

3.3. Heat transfer

Two models, *simple conductive* and *convective with a mobile bubble*, are investigated.

Simple conduction: the bubble is assumed to be motionless in the fluid with uniform surface temperature. The Fourier's law in spherical coordinates gives the heat flux Φ at the surface of the bubble: $\Phi = \left(\frac{k}{R_b(t)}\right)\left(T_b(t) - T_{b_0}\right)$ where k is the thermal conductivity (for water at $T_\infty = T_{b0} = T_0$ = 298.15K (25ºC), k = 0.6071 $W.m^{-1}K^{-1}$). The total heat transfer through the bubble surface S is equal to: $Q_{tot}(t) = S\Delta t\Phi = 4\pi R_b^2(t)\Delta t\left(\frac{k}{R_b(t)}\right)\left(T_b(t) - T_{b_0}\right)$. Starting from $t=0$ to $\Delta t = t$ after some arithmetic, and observing $\frac{T_b(t)}{T_{b_0}} = f^{3(1-m)}$, it comes: $Q_{tot}(t) = 4\pi Q_0 t\, f\left(f^{3(1-m)} - 1\right)$ with $Q_0 = k\, R_{b_0}T_{b_0}$.

Convective model with a mobile bubble: The motion of the bubble trough the flotation column creates a convective component for the heat transfer with water. Considering the bubble surface as isothermal, and applying the analytic method for laminar free convective heat transfer from isothermal spheres developed by [9], the heat flux at the surface bubble is: $\Phi = k\left(\frac{1}{R_b(t)} + \frac{1}{\sqrt{\alpha\pi t}}\right)\left(T_b(t) - T_{b_0}\right)$ where k is the thermal conductivity of the water, $\alpha = \frac{k}{\rho c_P}$ the thermal diffusivity, c_P the constant pressure heat capacity, $\rho = \frac{\rho_0}{1+\beta\left(T_b(t)-T_{b_0}\right)}$ the temperature dependent water density with at T_0 = 298.15K ρ_0=997.05 $kg.m^{-3}$, and β the water volumetric temperature expansion coefficient β =2.10$^{-4}K^{-1}$. After some arithmetic, it comes: $\Phi = k\, R_{b_0}^{-1} f\, T_{b_0}\left(f^{3(1-m)} - 1\right)\Phi_c$ with $\Phi_c = f^{-1} + \frac{R_{b_0} f\sqrt{c_P\rho_0}}{\sqrt{k\pi t\left(1+\beta T_{b_0}\left(f^{3(1-m)}-1\right)\right)}}$, being the convective term. Thus, the total heat transfer is given by $Q_{tot}(t) = 4\pi Q_0 t\, f\left(f^{3(1-m)} - 1\right)\Phi_c$, this expression is similar to the conductive case, excepted that it is multiplied by the convective term Φ_c.

4. Numerical simulation

Numerical simulations were made using the following parameters ([9], [7]): P_0=0.142MPa, σ=0.0728$N.m^{-1}$, R_{b0}=500-700μm, $\omega\tau_0$=-0.374, R/R_0=1, ω =28.5kHz, m=1.2, μ=0, ν=1, μ=0.025$N.s.m^{-2}$, ρ=1,800$kg.m^{-3}$, T_0=298.15K, n=1mol, $\Re$=8.314$J.mol^{-1}.K^{-1}$, and γ=1.4. Results are summarized Table 1.

4.1. Average temperature inside the bubble
Temperature inside a single bubble submitted to ultrasonic waves was calculated over a period against time (ωt), and fluctuates as a sinusoid (Figure 3a). Due to the compression of the gas, instantaneous temperature can reach punctually values as high as *300℃*, but also decrease under *0℃* during decompression. The average value of the temperature $\widetilde{T_b} = \frac{1}{2\pi}\int_0^{2\pi} T_b(\omega t)d(\omega t)$ was calculated by integration over one period of time. For the polytropic gas model, $\tilde{T}_b^P = 334.77K = 61.62°C$, a value corresponding approximately to one third less than for the ideal gas model ($\tilde{T}_b^I \approx 88.02$°C). Keeping the key parameters in the range $0 < \varrho < 1$ and m=1.2, prevents singularities for the bubble behavior and shows that the instantaneous temperature of the bubble is always inferior to 600K (not thousand of degrees as reported in [15]).

4.2. Average pressure inside the bubble
Pressure in the bubble fluctuates also as a sinusoid (Figure 3b), over a range of about *0.10MPa* given the boundaries conditions used for the reported numerical experience. The SRK and PR gas models give identical results with bigger amplitude variations compared to the ideal gas model. The average value of the bubble pressure $\widetilde{P_g} = \frac{1}{2\pi}\int_0^{2\pi} P_g(\omega t)d(\omega t)$ calculated by integration over one period of time is $\tilde{P}_g^{SRK} = 0.124MPa$ for the Peng-Robinson gas model and $\tilde{P}_g^I = 0.158MPa$ for ideal gas model.

4.3. Average internal work and head transfer between the bubble and the liquid
The *average wor*k done over a period by a bubble of radius equal to *500-700µm* has been estimated at $\widetilde{W}_{tot}^{Ig} = 4.95 - 13.58{\times}10^{-5}J$ for the ideal gas model, and at $\widetilde{W}_{tot}^{SRK/PR} = 3.64{-}10.00{\times}10^{-3}J$ for the Peng-Robinson gas model. The huge difference between the two models is in part explained by the higher power term affecting *f* in the Peng-Robinson model. The conduction model gives an average heat transfer of $\widetilde{Q}_{tot}^{Ig} = -8.08 - 22.18{\times}10^{-3}J$.

5. Thermodynamics variation against *m* and *ϱ*

5.1. Effect of polytropic coefficient m on P, T, ΔU, W_{tot}, Q_{tot},
P and T: Bubble average temperature and pressure increase when the process moves from isothermal to adiabatic (isentropic or reversible) both for the ideal and SRK gas model. Numerical results show unrealistic temperature and pressure for values greater than $m \approx 1.21$ (Figure 4a), indicating that heat and work flows in opposite directions ($\delta Q/\delta W > 0$), and the compression/decompression of bubbles would be closer to an isothermal than adiabatic process. The isothermal process (*m=1*) can be excluded, as heat is transferred through the bubble boundary from gas to the water given the thermal conductivity of water, so *m* would be in the range $1<m<1.21$. High values near the adiabatic conditions ($\Delta U \approx 0$) indicate that energy does not escape but accumulates in the bubble, increasing dramatically both the temperature and the pressure.

5.2. Effect of ultra sonic wave amplitude ϱ
Assuming a range $0 < \varrho < 1$ for the amplitude coefficient of the ultra sonic wave [7], and a polytropic process for an ideal or SRK gas, the temperature and pressure increase when the amplitude increases. For $0 < \varrho < 0.5$, the temperature inside the bubble increases smoothly with ϱ up to about 100°C, to reach a sharp increase up to 300°C for $\varrho \approx 0.8$, as more energy is carried by the ultrasonic wave . The over-pressure inside bubble also increases with ϱ from approximately *0.1* to *0.22MPa*.

5.3. Effect of polytropic coefficient m on thermodynamics
Internal energy ΔU_I (ideal gas model), total work W_{tot} (SRK gas model), and heat exchanges Q_{tot} (convective exchanges) have been calculated at the bubble scale over one period of time (Figure 5). As for average inside bubble temperature and pressure, they all reach high values nearby adiabatic conditions for ($m> 1.21$).

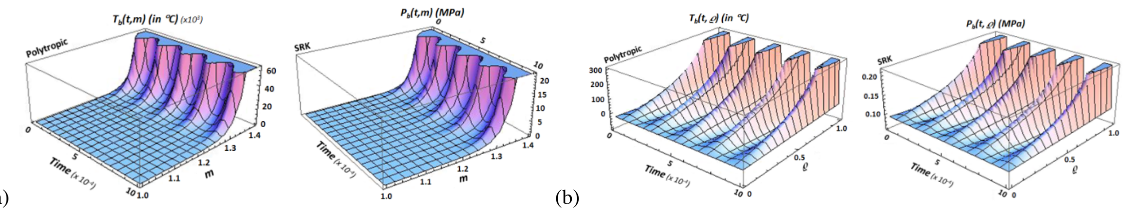

(a) Temperature Pressure (b) Temperature Pressure

Figure 4. Calculated temperature and pressure inside a bubble for polytropic and SRK models varying (a) the polytropic coefficient *m* and (b) the amplitude ϱ of the ultra sonic wave.

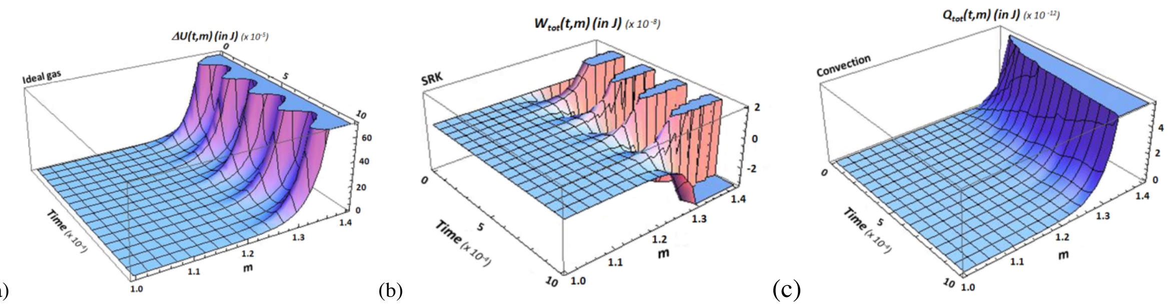

(a) Variation of bubble internal energy ΔU (b) Total work W_{tot} (c) Total convective heat exchange Q_{tot}

Figure 5. Calculated energy balance for polytropic and SRK models varying the polytropic coefficient *m* *(for* $R_0=13\mu m$*)*.

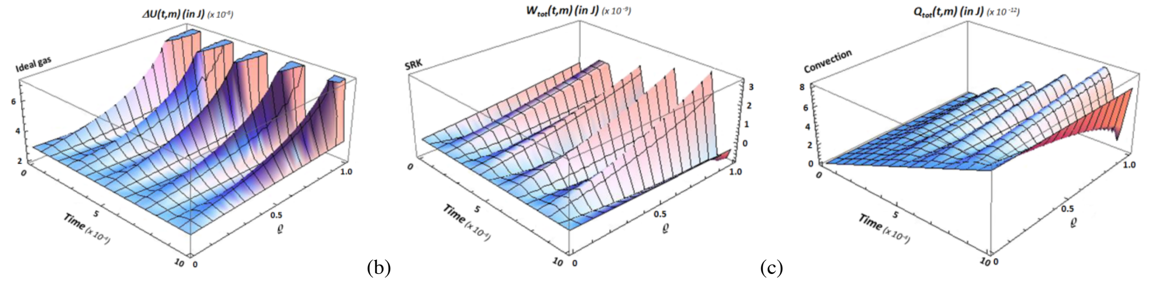

(a) Variation of bubble internal energy ΔU (b) Total work W_{tot} (c) Total convective heat exchange Q_{tot}

Figure 6. Calculated energy balance for polytropic and SRK models varying amplitudes ϱ of ultra sonic wave *(for* $R_0=13\mu m$*)*.

5.4. Effect of ultra sonic wave amplitude ϱ on thermodynamics

The same energy balance was performed when varying the ultrasonic amplitude ϱ (Figure 6). As for average inside bubble temperature and pressure, the internal energy and total work increase as amplitude increases. For the ideal gas model, the total work and total heat transfer are similar, but differ when applying a convective model of heat exchange (and SRK gas model). In this last case, the total heat seems to increase against time, indicating that the cooling of the bubble by the surrounding liquid is too slow, leading to an overheating of the gas trapped in the bubble.

6. Conclusions

This theoretical work demonstrates that the ultrasound effect on thermodynamics variables describing the temperature, pressure, internal energy, total work, and heat exchanges can be predicted at the bubble scale. The most direct impact is that under ultra sonic stimulation, the work required to modify the bubble volume is converted into heat that increases the average temperature of the gas trapped in the bubble, up to about *60℃*, or more, depending on the ultrasonic wave amplitude, the nature of the gas and the process involved (isothermal or adiabatic). This heat is transferred to the surrounding liquid by conduction (or convection) through the bubble surface, maintaining average bubble temperature equilibrium by cooling. However, given the micro bubble size, the warming of the surrounding liquid is limited at about 2°C, despite than nearby the bubble boundary, higher temperatures can be observed, implying in some case, the vaporization of the liquid, and thus the growing of the bubble. Inside bubble pressure increases by about 0.14MPa. Several assumptions have done during this theoretical work which may to be confirmed or not by experimental work, or by direct measurements of the bubble characteristics. The isothermal case is a very interesting case, because it induces a null internal energy, meaning that all the work done by the pressure forces on the bubble is integrally converted into heat supplied to the liquid around the bubble, without any lost due to the bubble heating/cooling, limiting the overall energy consumption due to ultrasonic stimulation. This favorable case should be searched when running a flotation process. Some authors suggest [12] the gas contained in the bubble does not correspond to a unique gas (air), but rather to a mixing of air and vapor created by boiling of the liquid surrounding the bubble. In this last case, it is required to take into account the energy used to vaporize the liquid in the energy balance, which is according to [12] higher than the energy used for heating/cooling the bubble, a point not investigated in this work.

7. Acknowledgements

The authors would like to express their thanks for the support to the Lorraine-Russia Arcus Project. The work was supported by the Russian Foundation for Basic Research (grant 17-41-590974).

References

[1] Clingan B V and McGregor D R 1987. *Column flotation experience at Magma Copper Company, with related experience of other mineral processors*, 116th Annual AIME-SME Meeting. Denver.

[2] Villar del R, Bouchard J, Desbiens A and Poulin E 2015. *Recent Developments in Flotation Column Instrumentation and Control: An Update*. Proceedings of the World Congress on Mechanical, Chemical, and Material Engineering (MCM 2015), Barcelona, Spain, July 20-21, Paper No. 127, 1-9.

[3] Kursun H and Ulusoy U 2015. Zinc Recovery from a Lead-Zinc-Copper Ore by Ultrasonically Assisted Column Flotation. *Particulate Science and Technology*, **33**(4), 349-356.

[4] Mosai R and Dawe R A 2003. Gas attachment of oil droplets for gas flotation for oily wastewater cleanup. *Separation and Purification Technology*, **33**(3), 303-314.

[5] Sobhy A 2013. *Cavitation nanobubble enhnaced flotation process for more efficient coal recovery*. PhD dissertation, Mining Engineering, University of Kentucky, UKnowledge, Lexington, US, 169p.

[6] Manlapig E V, Green C, Parkinson J W and Murphy A S 2001. *The technology and economic incentives for recovering coal from tailings impoundments*. SME Annual Meeting, Denver, Colorado, 26–28 February, Preprint 01-70.

[7] Royer J J, Filippov L O and Filippova I. V. 2012. *Improving fine mineral ore flotation using ultrasound*. Internal report, GeoRessources, Nancy, France, 22p.

[8] Filippov L O, Royer J J and Filippova I V 2016. *Improving efficiency in flotation ore recovery using ultra-sonic cavitation bubbles. Part I.* (this volume), 9p.

[9] Kim K and Kwak H Y 2007. Predictions of bubble behavior in sulfuric acid solutions by a set of solutions of Navier-Stokes equations. *Chemical Engineering Science*, **62**, 2880-2889.

[10] Foteinopoulou K and Laso M 2010. Numerical simulation of bubble dynamics in a Phan-Thien-Tanner liquid: non-linear shape and size oscillatory response under periodic pressure. *Ultrasonics*, **50**, 758-776.

[11] Nguyen A V, Ralston J and Schulze H J 1998. On modelling of bubble-particle attachment probability in flotation, *Int. J. Miner. Process*, **53**, 225-249.

[12] Brennen C E 1995. *Cavitation bubble dynamics*. Oxford University Press. 254p.

[13] Plesset M S and Zwick S A 1952. A Nonsteady heat diffusion problem with spherical symmetry. *Journal of applied physics*, **23**, 95-98.

[14] Carslaw H S and Jaeger J C 1959. *Conduction of heat in solids*. Oxford Univ. Press, 517p.

[15] Qi B and Aldrich C 2002. Effect of ultrasonic treatment on zinc removal from hydroxyde precipitates by dissolved air flotation. *Minerals Engineering*, **15**, 1105-1111.

[16] Beychok M R 1967. *Aqueous Wastes from Petroleum and Petrochemical Plants* (1st ed.). John Wiley & Sons Ltd. LCCN 67019834. 370p.